

than those of the corresponding motions in poly(ethylene terephthalate) (PET). Thus, $T > T_g$ annealing of PBT improves packing in the amorphous regions, lowers the average frequency of megahertz-regime cooperative main-chain motions, and lowers the methylene carbon $\langle T_{1\rho} \rangle$. This is in contrast to the $T < T_g$ annealing of PET,¹⁹ which lowers the frequency of main-chain motions already in the low-kilohertz regime and so increases the methylene carbon $\langle T_{1\rho} \rangle$. In addition, unlike the situation for PBT, protonated aromatic carbon dipolar sideband patterns²⁰ and ²D quadrupolar line shapes²¹ show that at room temperature none of the rings of quenched PET are flipping, at least at frequencies of 10^4 Hz or more. However, the average ring-oscillation frequency is still greater than 50 kHz. Thus, $T < T_g$ annealing increases spectral density at the rotating-frame Larmor frequency for the ring carbons of PET and shortens $\langle T_{1\rho}(C) \rangle$,¹⁹ opposite to the effect of $T > T_g$ annealing on PBT in which loss of the ring-flip population dominates relaxation. Finally, annealing at $T < T_g$ has no observable effect on amplitudes of either ring or methylene carbon motions in PET as judged by unchanged dipolar sideband patterns.²⁰ This means the observed changes in PET relaxation rates due to $T < T_g$ annealing are primarily due to changes in the frequencies rather than amplitudes of motion. This is not the situation for the $T > T_g$ annealing of PBT, as discussed in the following section.

Asymmetry and Main-Chain Motions in PBT. The asymmetry in the main-chain motion of the shorter $T_1(C)$ component of annealed PBT is apparent in differences in the $-\text{CH}_2-$ and $-\text{OCH}_2-$ dipolar patterns (Figure 4, right, and Table III, rows 8 and 9). The interior methylene carbon pattern is the more motionally averaged of the two, consistent with the results of ²D NMR experiments.² These differences do not appear for the quenched material (Figure 4, left). This means the constraints of tight interchain packing in, or the influence of microcrystalline domains on, the amorphous regions must be responsible for the asymmetry. In the loosely packed quenched PBT, major asymmetry in the amplitudes of methylene carbon motion is not prominent at room temperature, although

minor asymmetry is present as indicated by slight differences in $\langle T_{1\rho}(C) \rangle$'s and $\langle T_1(C) \rangle$'s (Tables I and II). The results of Figure 4 emphasize that the Helfand^{3,4} three-bond motion, which has been invoked to explain asymmetry in the methylene carbon motion,² should not be considered in terms of an isolated single chain in a vacuum, but rather in terms of a chain embedded in an interactive matrix.

Registry No. PBT (SRU), 24968-12-5; PBT (copolymer), 26062-94-2; $(\text{H}_3\text{CO})_2\text{C}_6\text{H}_4$, 27598-81-8; $[2-^{13}\text{C}]$ glycine, 20220-62-6.

References and Notes

- (1) Chollis, A. L.; Dumais, J. J.; Engel, A. K.; Jelinski, L. W. *Macromolecules* **1984**, *17*, 2399.
- (2) Jelinski, L. W.; Dumais, J. J.; Engel, A. K. *Macromolecules* **1983**, *16*, 492.
- (3) Helfand, E.; Wasserman, Z. R.; Weber, T. A. *J. Chem. Phys.* **1980**, *73*, 526.
- (4) Helfand, E.; Wasserman, Z. R.; Weber, T. A.; Skolnick, J.; Runnels, J. H. *J. Chem. Phys.* **1981**, *75*, 4441.
- (5) Schaefer, J.; McKay, R. A.; Stejskal, E. O.; Dixon, W. T. *J. Magn. Reson.* **1983**, *52*, 123.
- (6) Schaefer, J.; Sefcik, M. D.; Stejskal, E. O.; McKay, R. A.; Dixon, W. T.; Cais, R. E. *Macromolecules* **1984**, *17*, 1107.
- (7) Schaefer, J.; Stejskal, E. O.; McKay, R. A.; Dixon, W. T. *Macromolecules* **1984**, *17*, 1479.
- (8) Schaefer, J.; Stejskal, E. O.; Perchak, D.; Skolnick, J.; Yaris, R. *Macromolecules* **1985**, *18*, 368.
- (9) Schaefer, J.; Stejskal, E. O. *Top. Carbon-13 NMR Spectrosc.* **1979**, *3*, 284.
- (10) Stejskal, E. O. U.S. Patent 4446 430, May 1, 1984.
- (11) Torchia, D. A. *J. Magn. Reson.* **1978**, *30*, 613.
- (12) Schaefer, J.; Sefcik, M. D.; Stejskal, E. O.; McKay, R. A. *Macromolecules* **1984**, *17*, 1118.
- (13) Munowitz, M. G.; Griffin, R. G. *J. Chem. Phys.* **1982**, *76*, 2848.
- (14) Burum, D. P.; Linder, M.; Ernst, R. R. *J. Magn. Reson.* **1981**, *44*, 173.
- (15) Spiess, H. W. *Colloid Polym. Sci.* **1983**, *261*, 193.
- (16) Jelinski, L. W.; Dumais, J. J.; Watnick, P. I.; Engel, A. K.; Sefcik, M. D. *Macromolecules* **1983**, *16*, 409.
- (17) Yokouchi, M.; Sakakibara, Y.; Chatani, Y.; Tadokoro, H.; Tanaka, T.; Kentaro, Y. *Macromolecules* **1976**, *9*, 266.
- (18) Greenfield, M. S.; Vold, R. L.; Vold, R. R. *J. Chem. Phys.* **1985**, *83*, 1440.
- (19) Sefcik, M. D.; Schaefer, J.; Stejskal, E. O.; McKay, R. A. *Macromolecules* **1980**, *13*, 1132.
- (20) Schaefer, J., unpublished data.
- (21) Vega, A. J., unpublished data.

Theory of Polydispersity Effects on Polymer Rheology. Binary Distribution of Molecular Weights

Michael Rubinstein[†] and Eugene Helfand*

AT&T Bell Laboratories, Murray Hill, New Jersey 07974

Dale S. Pearson

Corporate Research Laboratories, Exxon Research and Engineering Company, Annandale, New Jersey 08801. Received August 1, 1986

ABSTRACT: Effects of polydispersity on rheological properties of entangled polymers are analyzed. A number of models of tube renewal are discussed and compared with each other and with experiments. A theory incorporating reptation, tube renewal, and fluctuations in the tube length into a general description of stress relaxation is developed. Dynamical moduli were calculated for monodispersed and bidispersed systems and compared with experiments. The product of viscosity and recoverable shear compliance is predicted to be of the order of the longest relaxation time of the higher molecular weight component with a weak dependence on the relative volume fraction of the binary mixture for a large enough concentration of longer molecules.

I. Introduction

Polydispersity has a profound effect on the viscoelastic properties of polymers. This is to be expected, since the

fundamental relaxation times in the system, the reptation times of the molecules, vary as a high power of molecular weight.

In this paper we explore some theoretical aspects of polydispersity, in particular its effects on the stress relaxation and dynamical moduli, and compare the theo-

[†] Present address: Research Laboratories, Eastman Kodak Co., Rochester, NY 14650.

retical predictions with experiments. Attention is confined to a system that is bimodal in its molecular weight distribution, i.e., to a mixture of short (S) and long (L) macromolecules. Their molecular weights, M_S and M_L , respectively, are well above the entanglement threshold; ϕ_S and ϕ_L are their weight fractions.

Struglinski and Graessley¹ have reported on dynamical moduli measurements of various binary mixtures of linear polybutadienes, with nearly monodispersed molecular weights of 40 700, 97 500, 174 000, and 435 000. They have examined some of the trends in the data and interpreted them using ideas presented earlier by Graessley² as well as some we present below. We concentrate here on understanding the physics that is revealed in their results, using as an example primarily one particular measurement on a mixture with $M_S = 40\,700$, $M_L = 435\,000$, $\phi_S = 0.44$, and $\phi_L = 0.56$.

Dynamical modulus curves for a nearly monodispersed sample of polybutadiene with molecular weight 430 000 are also discussed. These data and the experiments will be described more fully elsewhere.³

In the Doi-Edwards theory,⁴ each molecule is regarded as confined effectively to a tube by entanglements with the surrounding molecules. These tubes are considered permanent, or at least long-lived compared with other relaxation processes. The orientational state of the tube is partially imposed on the entrapped molecule. Relaxation occurs by escape from the initial tube as a result of reptation. This picture is insensitive to the nature of the molecules making up the tube. The molecules relax independently, so the relaxation modulus (in the terminal region) is predicted to be a linear combination of the moduli of the individual molecules

$$G(t) = G_N^\circ [\phi_L \mu(t/\tau_{RL}) + \phi_S \mu(t/\tau_{RS})] \quad (\text{I.1})$$

where G_N° is the plateau modulus (independent of molecular weight) and $\mu(t/\tau_{RK})$ represents the fraction of polymer of molecular weight M_K (reptation time τ_{RK}) that has not escaped from the initial tubes at time t . Theoretically, μ is given by⁴

$$\mu(t/\tau_{RK}) = \frac{8}{\pi^2} \sum_{p \text{ odd}} \frac{1}{p^2} \exp\left(-\frac{p^2 t}{\tau_{RK}}\right) \quad (\text{I.2})$$

and the reptation time τ_{RK} for molecules of type K is

$$\tau_{RK} \propto M_K^3 \quad (\text{I.3})$$

The dynamical loss modulus is related to the relaxation modulus by

$$G''(\omega) = \omega \int_0^\infty dt G(t) \cos(\omega t) \quad (\text{I.4})$$

In Figure 1 we compare the prediction of eq I.1 with the observed dynamical loss modulus data for the text mixture. The general two-peak structure is shown, indicating important processes with relaxation times τ_{RS} and τ_{RL} , but the heights of the peaks are grossly incorrect.

We believe that an important factor neglected is tube renewal, the release of constraints by virtue of surrounding molecules moving away. New constraints form as new molecules are encountered, but they confine a partially relaxed state. Molecules move away from the central one on the reptation time scales, τ_{RS} or τ_{RL} , so they should also contribute to the peaks at about the corresponding frequencies, $1/\tau_{RS}$ and $1/\tau_{RL}$. The importance of tube renewal processes in stress relaxation was pointed out by Graessley,² who explained thereby the differences of relaxation between linear molecules in a monodispersed melt and in a network. He also raised the issue of the effect

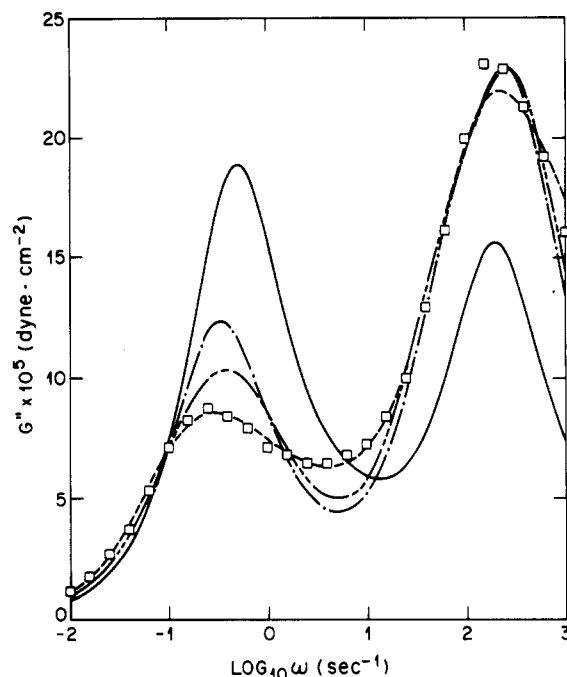


Figure 1. Dynamical loss modulus $G''(\omega)$ for a binary mixture of polybutadiene with molecular weights 40 700 and 435 000. Squares correspond to experimental points (ref 1). Solid curve is the best fit by the Doi-Edwards theory with no tube renewal. Dash-dotted curve is the fit by the theory incorporating reptation and tube renewal with the double- δ -function relaxation rate spectrum of eq II.9. Short-long dashed line is the fit by the theory with reptation and tube renewal modeled by random Rouse copolymer (cf. realistic spectrum of section II and Appendix). Short dashed line is the fit by the Marrucci-Viovy theory with reptation, tube renewal, and fluctuations. Parameters of the theoretical fits are given in Table I.

of tube renewal on polydispersed systems (experimental work of others on such samples is summarized in ref 1). In section II the tube renewal process will be discussed further and modeled.

In the tube model stress is considered to arise from orientational constraints imposed on each molecule by an effective tube, produced by the entanglements and deformed by strain. Relaxation occurs by escape from the tube constraints. As an end of a molecule first moves inward to some point in a deformed tube, the constraint of all outer parts of that tube becomes ineffective. This motion occurs by the reptation process, which may be treated primarily as Brownian motion of a molecule as a whole along its tube (i.e., at constant tube length). In an effort to explain the apparent $M^{3.4}$ dependence of viscosity, Doi⁵ considered the addition effect of relaxation by fluctuations in tube length. An implication of Doi's proposal is that more relaxation occurs at higher frequencies; i.e., the high-frequency side of a dynamic loss modulus peak should decrease less rapidly than predicted by pure reptation. These characteristics are evident in the data, so in section III Doi's approach to fluctuations will be incorporated into the model.

An important factor that must be considered in the development of a quantitative theory is the question of how many entanglements are released when a molecule from the surroundings moves away from a central molecule. This question is related to the controversial issue of the concentration dependence in solutions of the distance between entanglements and of the plateau modulus. We discuss various views on the matter in section IV but finally resort to choosing an empirical power-law concentration dependence to fit the data.

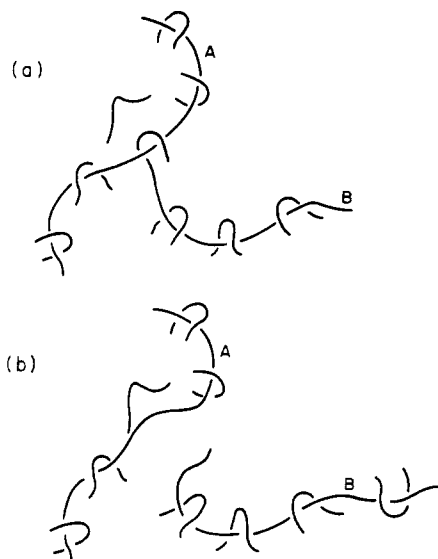


Figure 2. Molecules A and B go from an entangled (a) to a disentangled (b) state. Thereby molecule B relaxes a segment completely by reptation, while molecule A relaxes a segment partially by tube renewal.

While working on the present paper, we received preprints on tube renewal by Marrucci⁶ and Viovy.⁷ In section V we describe their theories and incorporate them into some of our models.

In section VI we compare the various theoretical approaches with data and discuss the results.

II. Tube Renewal

Figure 2 depicts schematically two molecules (more precisely, the molecules' primitive paths) and several confining entanglements with surrounding molecules. Relaxation by reptation occurs when the end of molecule B passes (disentangles from) molecule A. Relaxation of molecule A by tube renewal occurs when a surrounding molecule B's end disentangles from the A molecule.

It is clear that the number of reptative disentanglements is equal to the number of tube renewal processes. Every reptative disentanglement for one molecule is a tube renewal disentanglement for another, but the stress relaxation associated with each process is different. A reptative disentanglement allows the orientation of the end segment of molecule B to relax completely, i.e., to assume all orientations with equal probability. However, the tube renewal disentanglement allows the orientation of the freed segment of the molecule A to relax only to the extent allowed by the adjacent segments along chain A.

Tube renewal processes occur on the time scale of the reptation time of the surrounding molecules, which is τ_R if the molecules have the same molecular weight. This allows the freed segment of the central molecule to move for a distance of order a , the distance between entanglements. A sequence of such steps can be regarded as Brownian motion with the diffusion constant

$$D_e = a^2/6\tau_R \quad (\text{II.1})$$

and the effective friction constant, ζ , for a segment

$$\zeta = \frac{k_B T}{D_e} = \frac{6k_B T \tau_R}{a^2} \quad (\text{II.2})$$

Since the segments are attached, it is necessary to consider the Brownian motion of the whole molecule with its many degrees of freedom. For this purpose, the Rouse theory can be used. Alternatively, as was suggested earlier,² a Rouse-like spectrum of relaxation times also arises from

an Orwoll-Stockmayer conformational flip model.⁸

To describe the spectrum of relaxation rates associated with tube renewal, we adopt a model wherein each segment of the tube is associated with an entanglement and has a fixed relaxation time. For a monodispersed system, one may take all of these times as equal, τ . We will later set $\tau = \kappa\tau_R$, with the expectation that κ is a number of order unity. Graessley has proposed a model² whereby several entanglements are to be associated with a given segment, and the first to release allows relaxation to occur. Such a model, or a variety of others, can be embodied in κ . Also, κ can account for the small effect due to the fact that relaxation by reptation is not described by a single-exponential time decay (Poisson process).

From the Rouse theory, one finds that the central portion of the tube relaxes by tube renewal according to the law

$$R(t) = \frac{1}{N} \sum_{j=1}^N \exp(-\epsilon_j t) \quad (\text{II.3})$$

where

$$\epsilon_j = \frac{4}{\tau} \sin^2 \left[\frac{\pi j}{2(N+1)} \right], \quad j = 1, \dots, N \quad (\text{II.4})$$

For large N and $t \ll N^2\tau$, the sum over j can be replaced by an integral over relaxation rates, ϵ

$$R(t) = \int_0^\infty d\epsilon \rho(\epsilon) \exp(-\epsilon t) \quad (\text{II.5})$$

with a density of relaxation rates given by

$$\rho(\epsilon) = \frac{d(j/N)}{d\epsilon} = \frac{1}{\pi} \left[\frac{\tau}{\epsilon(4 - \epsilon\tau)} \right]^{1/2}, \quad \epsilon\tau < 4$$

$$= 0, \quad \epsilon\tau > 4 \quad (\text{II.6})$$

Relaxation is to be regarded as occurring by the two parallel mechanisms, reptation and tube renewal. Reptation destroys all constraining effects of a portion of the tube, leaving at time t only an average fraction $\mu(t)$ of the tube maintaining the original affine distortion. The stress arising from this undestroyed portion is not G_N° , the plateau modulus, as in the Doi-Edwards theory, but only a fraction $R(t)$ of that not relaxed by tube renewal

$$G(t) = G_N^\circ R(t) \mu(t) \quad (\text{II.7})$$

For a binary mixture, we will consider the following model to estimate the relaxation due to tube renewal. Assume that a fraction of the entanglements on a given chain, ϕ_{fast} , is associated with the fast release time $\tau_{\text{fast}} = \kappa\tau_R$ and that $\phi_{\text{slow}} = 1 - \phi_{\text{fast}}$ is associated with the longer time $\tau_{\text{slow}} = \kappa\tau_{\text{RL}}$. Each entanglement will be permanently associated, at random, with one or another of these times. The problem of relaxation by tube renewal would then be equivalent to Rouse relaxation of a random copolymer with beads (segments) characterized by one of two different friction constants (cf. Appendix). Thus for the i th bead $\zeta_i = \zeta_{\text{fast}}$ or ζ_{slow} , related to τ_{fast} or τ_{slow} by eq II.2. The spectrum of relaxation rates for a given assignment of friction constants is given by the eigenvalues of the matrix $2\gamma\zeta^{-1}\mathbf{A}$, where γ is the effective segment force constant, which we take as $3k_B T/a^2$; ζ is a diagonal matrix with the effective friction constant ζ_i of the i th segment in position i , and \mathbf{A} is the Rouse matrix with $A_{ii} = 2$ and $A_{i,i\pm 1} = -1$. (End conditions on \mathbf{A} are irrelevant, since the ends relax much faster by reptation. They may be chosen as cyclic for convenience.)

Dean⁹ has derived a formula for the relaxation spectrum, but the equation is difficult to solve and will not be used

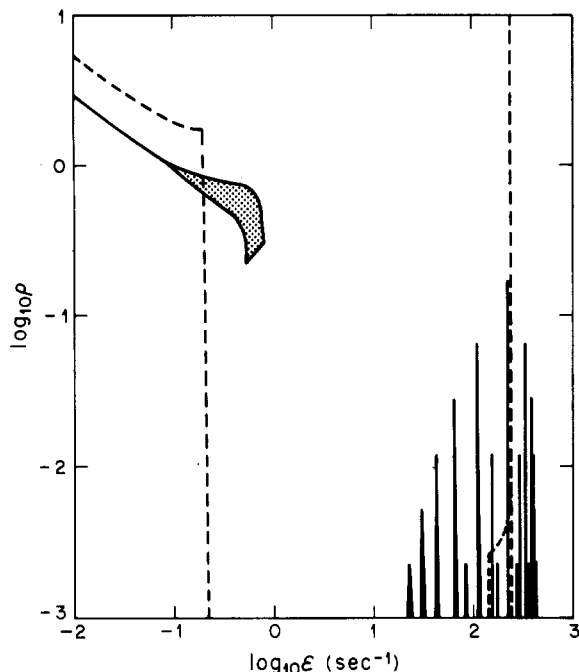


Figure 3. Relaxation rate spectrum $\rho(\epsilon)$. Solid curve is the Rouse model with random distribution of fast and slow beads (cf. Appendix) with concentration $\phi_{\text{fast}} = 0.56$ of fast ones. Dashed curve is the "split Rouse" spectrum for the same fraction of short-time modes (cf. eq II.8). The shading indicates that large statistical fluctuations in our simulation leave the exact spectral density in this region uncertain, but with negligible observable effect on the modulus.

here. Bear in mind that going from a relaxation spectrum to a stress modulus smears out details of the spectrum so that a particularly accurate determination is not essential.

The relaxation spectrum has been approximated by a method, details of which are presented in the Appendix. We will call it the "realistic" spectrum. The method is based on the following physical argument, valid when $\tau_{\text{RL}} \gg \tau_{\text{RS}}$. On the time scale for motion of a low-friction segment the high-friction segments are essentially immobile. Thus the high relaxation rate portion of the spectrum corresponds to the essentially discrete relaxation rates of short sequences of low-friction segments nearly isolated between fixed high-friction segments. The length of such a sequence is Poisson distributed, which determines the intensity of each peak. A sequence of n low-friction segments has n relaxation rates corresponding to the n Rouse modes. The high- ϵ part of the spectrum, depicted in Figure 3, was obtained in this way.

With regard to the slow relaxation of the high-friction segments, the rapidly relaxing segment sequences between them serve as effective springs. The corresponding spring constant is inversely proportional to the sequence length plus one. Thus the problem of the slow relaxation modes corresponds to the Rouse relaxation of a chain of elements all with friction constant ζ_{slow} but with force constants that are statistically distributed. The low- ϵ part of the spectrum was determined by a computer simulation of such a stochastic problem using a method of Dean.⁹ The results are depicted in Figure 3. The statistical noise (due to the finite sample) at the high- ϵ end of the low- ϵ band is of little significance because of the aforementioned smearing in conversion to a modulus.

One important feature of the spectrum, actually more general than this model of high- and low-friction segments, is that the ratio of the number of fast to slow modes (area under the corresponding portion of the spectrum) is $\phi_{\text{fast}}/\phi_{\text{slow}}$. This observation can be made the basis for

simpler, but less accurate, models. These models capture essential aspects of the physics of tube renewal with rapidly and slowly relaxing entanglements. In a Rouse model with uniform friction the modes have eigenstates that are waves of nodal spacing Na/j along the chain. We now assume that the motion of the entanglements and their relaxations are such as to allow the ϕ_{fast} Rouse modes with nodal spacing less than a/ϕ_{slow} to relax with characteristic time τ_{fast} , while the remaining modes relax with time τ_{slow} . The relaxation spectrum is then like eq II.6, but with a split scale of relaxation rates

$$\rho(\epsilon) = \frac{1}{\pi} \left[\frac{\tau_{\text{slow}}}{\epsilon(4 - \epsilon\tau_{\text{slow}})} \right]^{1/2}, \quad \epsilon < \frac{4}{\tau_{\text{slow}}} \sin^2 \left(\frac{\pi}{2} \phi_{\text{slow}} \right)$$

$$\rho(\epsilon) = 0, \quad \frac{4}{\tau_{\text{slow}}} \sin^2 \left(\frac{\pi}{2} \phi_{\text{slow}} \right) < \epsilon < \frac{4}{\tau_{\text{fast}}} \sin^2 \left(\frac{\pi}{2} \phi_{\text{slow}} \right)$$

$$\rho(\epsilon) = \frac{1}{\pi} \left[\frac{\tau_{\text{fast}}}{\epsilon(4 - \epsilon\tau_{\text{fast}})} \right]^{1/2}, \quad \frac{4}{\tau_{\text{fast}}} \sin^2 \left(\frac{\pi}{2} \phi_{\text{slow}} \right) < \epsilon < \frac{4}{\tau_{\text{fast}}}$$

$$\rho(\epsilon) = 0, \quad \frac{4}{\tau_{\text{fast}}} < \epsilon \quad (\text{II.8})$$

as illustrated by the dashed line in Figure 3.

Simpler yet, for a rough approximation, the two bands of the spectrum can each be collapsed to a single relaxation rate, and the spectrum can be written with just the two characteristic times

$$\rho(\epsilon) = \phi_{\text{slow}} \delta \left(\epsilon - \frac{1}{\tau_{\text{slow}}} \right) + \phi_{\text{fast}} \delta \left(\epsilon - \frac{1}{\tau_{\text{fast}}} \right) \quad (\text{II.9})$$

which leads to

$$R(t) = \phi_{\text{slow}} \exp \left(-\frac{\tau}{\tau_{\text{slow}}} \right) + \phi_{\text{fast}} \exp \left(-\frac{t}{\tau_{\text{fast}}} \right) \quad (\text{II.10})$$

The extra spectral broadening associated with the distribution of characteristic size of the modes is lost.

The dynamical loss moduli $G''(\omega)$ calculated by using the "realistic" spectrum (solid line in Figure 3) and by using the δ -function spectrum of eq II.9 are compared with experiment in Figure 1. We have set $\phi_{\text{fast}} = \phi_S$. There is a large improvement over the Doi-Edwards fit (solid curve in Figure 1). In particular, there is much more loss at high frequencies. This is because not only does all the stress contributed by the short chains relax at rates of order $1/\tau_{\text{fast}}$, but a fraction ϕ_{fast} (taken as ϕ_S for the moment) of the long chain stress relaxes with the same characteristic rate by tube renewal.

Several features of the theoretical fit are still less than satisfactory. The high-frequency sides of the two peaks do not have the correct shape. Also, the height of the peaks (more properly, the area under the peaks) is not quite right. We address these issues in the following sections.

In view of these two difficulties, it is hard to judge how good a model of the tube relaxation spectrum one needs to use. Note that the δ -function spectrum does not do a good job on the low-frequency sides of the loss peaks. One is inclined to use one of the spectra with some width, since these are better on the low-frequency side and marginally better throughout.

III. Relaxation by Fluctuations in Tube Length

In the Doi-Edwards theory,⁴ escape from the tube is assumed to occur primarily by Brownian motion of the molecule as a whole along the tube axis. Fluctuations that

shorten the tube (alternatively, the primitive path) can lead to additional relaxation near the tube's ends, i.e., destruction of tube constraints. However, the contribution to the viscosity, for instance, is a term of $O(N^{-1/2})$ smaller than without fluctuations. Doi has pointed out,⁵ however, that the number of segments of the tube is usually not so large that the fluctuation terms are irrelevant. The fluctuation processes occur on a shorter time scale than reptation, so they should be particularly important for dynamical loss at frequencies much larger than $1/\tau_R$.

Doi has analyzed these processes along the following lines.⁵ The length fluctuations occur with a Rouse spectrum of relaxation times up to the longest Rouse time $\tau_{eq} \approx N^2\tau_a$, where τ_a is the longest Rouse relaxation time of a single segment (a chain of N_e monomers). This leads to a root-mean-squared displacement along the tube of the polymer ends that grows like $t^{1/4}$. On the other hand, for times $t > \tau_{eq}$, the motion of the ends is dominated by the reptation of the molecular as a whole, but the molecule now acts as if it were shorter by an amount of the order of the range of mean length fluctuations. This led Doi to postulate as a function to describe the relaxation modulus

$$G(t) = G_N^\circ f_D(t/\tau_R)$$

$$f_D\left(\frac{t}{\tau_R}\right) = \int_0^1 d\xi \exp\left(-\frac{t}{\tau_\xi}\right) \quad (\text{III.1})$$

where

$$\frac{\tau_\xi}{\tau_R} = \frac{N}{16\nu^2\xi^4}, \quad \xi \leq \frac{2\nu}{N^{1/2}}$$

$$= \left(\xi - \frac{\nu}{N^{1/2}}\right)^2, \quad \xi > \frac{2\nu}{N^{1/2}} \quad (\text{III.2})$$

The $t^{1/4}$ initial decrease of the tube size by end fluctuations produces an $\omega^{-1/4}$ decrease of dynamical loss modulus on the high-frequency side of a loss peak (rather than the more rapid $\omega^{-1/2}$ decrease of the Doi-Edwards theory). The effect of this on fitting is discussed later; but, qualitatively, the extra high-frequency loss (slower high-frequency fall-off) is in accord with the experimental data in Figure 1. Even clearer verification comes from observations of the modulus of monodispersed samples, as discussed in Section VI.

IV. Concentration Dependence of Entanglement Density

Earlier, we defined ϕ_{fast} as a fraction of the entanglements of a given chain that relax on the fast time scale. We refrained from the assumption that this fraction is necessarily equivalent to the fraction of short chains. The relation of entanglement density or spacing to concentration has been a controversial issue in the literature, and a variety of laws and physical models have been proposed.

Ferry¹⁰ has reviewed experimental measures of the distance between entanglements from the plateau modulus, break point in the viscosity vs. molecules weight plots, and a variety of other measurements. Recent data are reported by Raju et al.¹¹ They write as an empirical law for the plateau modulus

$$G_N^\circ \propto \phi^\alpha \quad (\text{IV.1})$$

Assuming that the plateau modulus is proportional to the number of chain segments between entanglement per unit volume, one can write

$$G_N^\circ \propto \phi/N_e \propto \phi/a^2 \quad (\text{IV.2})$$

which implies

$$a \propto \phi^{-(\alpha-1)/2} \quad (\text{IV.3})$$

Experimentally α is found from plateau moduli to be between 2.0 and 2.3 (the a exponent would be between -0.5 and -0.65).

An α value of 2 was proposed by Kelley and Bueche,¹² and many later authors, by hypothesizing that the number of entanglements is proportional to the number of monomer-monomer contacts. The proportionality constant must be taken as quite small, of order 0.01, to be in accord with measurements. Evans and Edwards¹³ also find $\alpha = 2$ to be a consequence of the physical assumption that the entanglement spacing can be a function only of the length of polymer per unit volume. The result follows from a geometric argument or from dimensional analysis.¹⁴ Rubinstein and Helfand¹⁵ and Helfand¹⁴ reasoned that the spacing between entanglements should be a function of the length of the primitive path (rather than total polymer) per unit volume, which would imply $\alpha = 3$ ($a \propto \phi^{-1}$). Physically this means that a tube renewal of molecule A can occur when a reptating molecule C disentangles from a loop of molecule B, which thereby can release a segment of A.

Henceforth in this paper, the exponent α in eq IV.1, relating plateau modulus and concentration, will be left as a fitting parameter.

V. Tube Renewal Theories of Marrucci and Viovy

Marrucci advanced a simple means of approximating the effects of tube renewal on the viscoelastic properties of polymers.⁶ He proposed that tube renewal be regarded as effectively enlarging the diameter of the tube and the spacing between entanglements, a . In the Doi-Edwards formula (for monodispersed polymer)

$$G(t) = G_N^\circ \mu(t/\tau_R) \quad (\text{V.1})$$

a enters implicitly in two ways. We discussed in section IV the plateau modulus dependence on the spacing between entanglements $G_N^\circ \propto a^{-2}$ (cf. eq IV.1). Also, a enters the reptation time $\tau_R = L^2/\pi^2 D_R$ through $L = N_0 b^2/a$, where L is the tube length and N_0 is the number of monomers per chain. (The curvilinear diffusion constant along the tube $D_R = k_B T/N_0 \zeta$ is independent of a .) Marrucci assumes that a fraction $1 - \mu(t)$ of the original entanglements has been removed at time t , and similarly to the phenomenological concentration dependence $a_\phi = a_1 \phi^{-(\alpha-1)/2}$, he writes

$$a(t) = a(0)[\mu(t/\tau_R)]^{-(\alpha-1)/2} \quad (\text{V.2})$$

Let us examine the physical basis for the way a enters eq V.2. This will provide a means for judging the degree to which it is appropriate to use this relation.

First, consider the model introduced earlier for the bimodal distribution when there are two distinct and widely separated times. The contribution to the relaxation modulus from the long chains is

$$G_L(t) = \frac{4}{5} \frac{k_B T c_L b^2}{a^2} \exp\left(-\frac{t}{\tau_p}\right) \mu_L\left(\frac{t}{\tau_{slow}}\right) \quad (\text{V.3})$$

where p labels the modes, of which there are N_{0L}/N_e for a chain with N_{0L} monomers. Of these modes, a fraction $\phi_L^{\alpha-1}$ are slow and the rest are fast. Consider a time intermediate between the fast and slow relaxation times. Then $\exp(-t/\tau_p)$ is essentially zero for a fast mode and essentially unity for a slow one. Hence in this range

$$G_L(t) = \frac{4}{5} \frac{k_B T c_L b^2}{a^2} \phi_L^{\alpha-1} \mu_L(t/\tau_{RL}) \quad (\text{V.4})$$

Table I
Parameters for Theoretical Fits to Experimental Curves

fit ^a	no. of fitting parameters	$G_N^\circ \times 10^7$, dyn/cm ²	$\tau_1 \times 10^{-2}$	τ_2	N_1/ν^2	N_2/ν^2	α	κ
A	2	1.075		2.7				
B	3	1.09		9.8				0.25
C	3	1.208		13.2		44.3		
D	3	1.220		36.1		218		
E	3	0.807	0.496	2.05				
F	4	0.879	1.446	16.3				0.249
G	3	0.942	0.608	7.5				
H	4	0.929	1.64	10.8				0.271
I	5	1.195	2.56	44.1		64.2	2.254	
J	6	1.136	2.00	45.9	178.5	60.8	1.942	

^a A-D, monodispersed polybutadiene with molecular weight 430 000; E-J, bidispersed mixture with molecular weights $M_s = 40\,700$ and $M_L = 435\,000$ and volume fractions $\phi_s = 0.44$ and $\phi_L = 0.56$ A, Doi-Edwards theory; B, Doi-Edwards theory with Rouse tube renewal; C, Doi theory of reptation and fluctuations;⁵ D, Marrucci-Viovy theory with reptation, tube renewal, and fluctuations; E, Doi-Edwards theory; F, Doi-Edwards theory with double- δ -function tube renewal; G, Marrucci-Viovy theory with reptation and tube renewal but without fluctuations; H, Doi-Edwards theory with random Rouse copolymer tube renewal (cf. section II and Appendix); I, Marrucci-Viovy theory with reptation, tube renewal, fluctuations, and fixed ratio of molecular weights $N_2/N_1 = 10.68$; J, same as I but without the constraint (both N_1/ν^2 and N_2/ν^2 are treated as fitting parameters).

This formula is as if a in the plateau modulus were replaced by $a(t) = a\phi_L^{-(a-1)/2}$, as Marrucci proposed.⁶

In general, the observation time does not lie between two distinct time scales. If one writes $G(t) = G_N^\circ R(t)\mu(t)$, where R is to account for tube renewal, then Marrucci would have (with $\alpha = 2.2$)

$$R(t) = [\mu(t)]^{1.2} \quad (\text{V.5})$$

If $\mu(t)$ is dominated by a single exponential, as in the Doi-Edwards theory, then $R(t)$ decays as $\exp(-1.2t/\tau_R)$. This is much more rapid than the $t^{-1/2}$ tube renewal contribution to stress relaxation predicted by using a Rouse model, as above. Nevertheless, eq V.4 does handle processes well separated in time, and it is easy to use. Therefore, it will be tried in some of the curve fittings below.

The use of an a that enlarges with time in the formula for τ_R , as proposed by Marrucci,⁶ is another matter. Even though entanglement constraints are being released, new ones are constantly being formed. Therefore in the equation $\tau_R = L^2/\pi^2 D_R$, with $L = Na = N_0 b^2/a$, the contour length for the reptation process remains unchanged. The important point is that the tube renewal processes are slow on the time scale over which the chain reptates the distance of a single segment length, $N_0 \xi a^2/k_B T$. (By contrast, one does not set $L = N_0 b$ because, internally, single segments are relaxing rapidly on this time scale.)

This modification of Marrucci's argument to keep a constant in τ_R has been used by Viovy⁷ and independently by us for this work, and we will refer to the formula

$$G(t) = G_N^\circ [\mu(t)]^\alpha \quad (\text{V.6})$$

as the Marrucci-Viovy (MV) approximation. Although both Marrucci and Viovy used only the Doi-Edwards form for $\mu(t)$, we will incorporate into $\mu(t)$ the effects of the tube-length fluctuations according to eq III.1 and III.2.

VI. Dynamical Loss Modulus

To appreciate the relations of the various physical phenomena to the dynamical loss data, we will consider theoretical fits to experimental data of one monodispersed sample and one with a bimodal distribution of molecular weights (as described above).

One of the curves of Figure 4 shows a fit of the monodispersed-sample loss modulus to Doi's form of relaxation, eq III.1 and III.2, which includes the effect of tube-length fluctuations but no tube renewal. The curve fit is good, especially the fit of the high-frequency data, which show

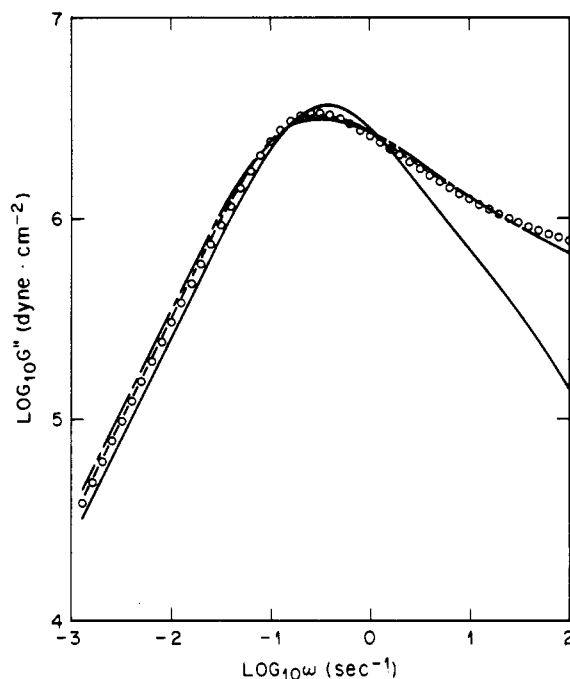


Figure 4. Dynamic loss modulus $G''(\omega)$ for monodispersed polybutadiene with molecular weight 430 000. Squares represent experimental points (ref 3). Solid curve is the best fit by the Doi-Edwards reptation theory with no tube renewal and no fluctuations. Short dashed curve is the fit by the Doi theory of reptation and fluctuations (ref 5). Short-long dashed line is the fit by the Marrucci-Viovy theory with reptation, fluctuations, and tube renewal.

an $\omega^{-1/4}$ behavior characteristic of the fluctuations. However, the fitting parameter $N/\nu^2 = 44.3$ is suspiciously low. For this sample, $N = (5/4)(M/M_e)$ is 290 (using $M_e = 1850$),¹ so $\nu = 2.6$. However, Doi has theoretically estimated ν to be 1.47.⁵ (Slight uncertainty is introduced into the fit in the high-frequency region, owing to yet higher frequency loss processes, such as those involved in relaxation of the primitive path length in the stretched tube and Rouse-like relaxation of the segments between entanglements.)

The above fit (short dashed lined in Figure 4) does not account for tube renewal. Taking tube renewal into account by means of the Marrucci-Viovy approximation (MV), eq V.6 with $\alpha = 2$, and using Doi's eq III.1 and III.2 again for tube length fluctuations, one gets the short-long dashed curve in Figure 4 with the parameters in Table I.

The value of N/ν^2 has now gone to 218, which corresponds to $\nu = 1.15$, perhaps too low. In this fit N/ν^2 went up because fluctuations make an additional contribution to relaxation by tube renewal. To make up for this missing process in the former fit, the fluctuations are made relatively more important by regarding the chain as shorter (smaller N/ν^2).

The relaxation modulus at long times decays as $\exp(-t/\tau_d)$ if one uses just Doi's eq III.1 and III.2 as opposed to $\exp(-2t/\tau_d)$ for MV, where $\tau_d = \tau_R(1 - \nu N^{-1/2})^2$ is the longest relaxation time in the Doi tube-fluctuation theory.⁵ This accounts for the larger τ_d in the latter fit.

To a considerable extent the effects of tube renewal on the shape of the modulus curves of monodispersed polymers can be absorbed into the values of the parameters. This may be why the importance of tube renewal was recognized only lately,² although the parameters were known to be anomalous.

As demonstrated in the Introduction, the effect of tube renewal on the modulus of a sample with a bimodal distribution of molecular weights is much more evident. Simple reptation predicts that for times intermediate between τ_{RS} and τ_{RL} the modulus should have a second plateau of height $\phi_L G_N^\circ$, which would correspond to the area under the low-frequency peak. This implies that all the stress in the short chains has relaxed, but none in the long ones. Tube renewal dictates that a fraction ϕ_{fast} of the stress in the long chains has also relaxed, so the second plateau value is $\phi_{slow} \phi_L G_N^\circ$. The factor ϕ_{slow} can be taken as $\phi_L^{\alpha-1}$ phenomenologically.

In section II, we demonstrated this effect easily in a fit of some data to a theory with $\alpha = 2$. We also saw that there was more loss on the high-frequency side of the peaks than predicted by the simple reptation theory, so fitting would require a functional form that included tube-length fluctuations in an adaptation of Doi's theory.⁵ We saw above that the effects of tube-length fluctuations on both end escape and tube renewal should be taken into account. This is most easily done with the MV theory. Thus we will investigate fits of the relaxation modulus to

$$G(t) = G_N^\circ [\phi_L f_D(t/\tau_{dL}, N_L) + \phi_S f_D(t/\tau_{dS}, N_S)]^\alpha \quad (\text{VI.1})$$

with f_D given by eq III.1 and III.2. Dynamical modulus data¹ for the sample with a binary distribution of molecular weights have been fitted to this form (Fourier transformed), with parameters given in Table I, and are shown in Figure 1. The values of N_L/ν^2 and N_S/ν^2 are completely anomalous. The data show the high-frequency side of the high-frequency peak falling off relatively faster than that of the low-frequency peak. Theory would say that for longer chains relaxation by tube-length fluctuations should have been less important so fall-off rates should be reversed from the observations. One must conclude that there is far too much relaxation at frequencies intermediate between $1/\tau_{RL}$ and $1/\tau_{RS}$ and/or there is too little relaxation for $\omega > 1/\tau_{RS}$. Further experimental studies directed to these frequency ranges are in progress.

Unfortunately, the inability to fit well the high-frequency sides of the peaks introduces an uncertainty in the parameter α . Note that the dashed curve in Figure 1 has a corresponding parameter $\alpha = 1.94$. However, other fits that forced the parameters for fluctuation effects to be more reasonable had $\alpha \approx 2.2$.

In ref 1 the data on the slow peak are analyzed in a different way so as to emphasize the central portion. The height of the peak is plotted vs. volume fraction of the long chain for a variety of bimodal blends. A $\phi_L^{2.26}$ dependence of the height of the peak fits the data rather well. However, we disagree with a prediction that the viscosity of the

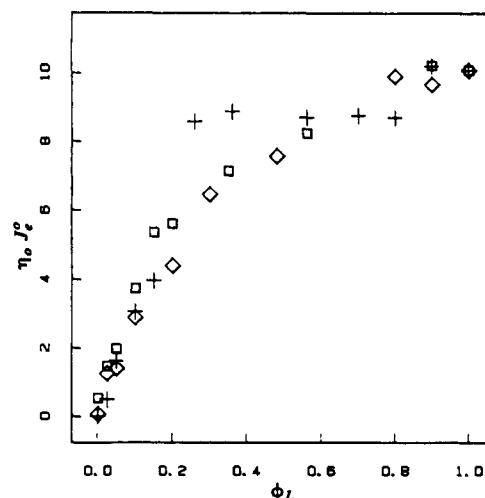


Figure 5. Products of zero-shear-rate viscosity η_0 and recoverable shear compliance J_e° of binary mixtures of polybutadiene are plotted as a function of the volume fraction of the higher molecular weight component. In all cases the longer molecules have molecular weight 435 000. Mixtures with the shorter molecules having molecular weight 40 700 are denoted by pluses, weight 97 500 by diamonds, and weight 174 000 by squares.

mixture should vary as the 3.4 power of the weight-average molecular weight, $\eta_0 \sim \bar{M}_w^{3.4}$, where $\bar{M}_w = \phi_S M_S + \phi_L M_L$. Since $M_L \gg M_S$ such a law would imply that, effectively, η_0 varies as $\phi_L^{3.4}$, which appears to be in disagreement with their data.

The zero-shear-rate viscosity is defined by

$$\eta_0 = \lim_{\omega \rightarrow 0} \frac{G''(\omega)}{\omega} = \int_0^\infty G(t) dt \quad (\text{VI.2})$$

and the recoverable shear compliance is

$$J_e^\circ = \frac{1}{\eta_0^2} \lim_{\omega \rightarrow 0} \frac{G'(\omega)}{\omega^2} = \frac{1}{\eta_0^2} \int_0^\infty t G(t) dt \quad (\text{VI.3})$$

Both viscosity and the compliance get dominant contribution from the time range $t \gg \tau_{RL}$. The product $J_e^\circ \eta_0$ is a characteristic time of the mixture weighted toward the longest times. For $\tau_{RL} \gg \tau_{RS}$ and ϕ_L not too small, this time should be equal to τ_{RL} with only a weak ϕ_L dependence:

$$J_e^\circ \eta_0 = \tau_{RL} U(\phi_L) \quad (\text{VI.4})$$

From the model where a fraction $(1 - \phi_L^\alpha)$ of the stress relaxes at the rapid rate one should find $J_e^\circ \propto \phi_L^{-\alpha}$ and $\eta_0 \propto \phi_L^\alpha$. Data for a variety of blends have been used to show that J_e° goes as $\phi_L^{-2.24}$ for ϕ_L high enough that the long molecules are well entangled with each other and dominate the viscosity.¹ In Figure 5 we demonstrate, using data from Struglinski and Graessley, that the product $\eta_0 J_e^\circ$ is a weak function of ϕ_L for high enough values of ϕ_L .

VII. Summary

To study the effects contributing to the viscoelastic properties of polydispersed polymer systems, we analyzed the dynamic loss modulus of a sample with a bimodal distribution of molecular weights. The fit of the loss curve by the Doi-Edwards theory⁴ is poor. The theory predicts much less loss at higher frequency than is experimentally observed. This means that the stress associated with the long chains is relaxing by tube renewal.

For times between τ_{RS} and τ_{RL} , there should be a second plateau. If entanglements with short molecules are regarded as totally relaxing on the time scale of reptation of the long molecules, then the second plateau modulus

should have the same dependence on ϕ_L as a solution of these molecules has on ϕ . A solution theory¹³ that says that the degree of entanglement depends only on the total length of polymer in the system has $G_N^0 \propto \phi^2$. A theory¹⁵ that says that the degree of entanglement depends on the total length of the primitive path has $G_N^0 \propto \phi^3$. Phenomenologically, one can write $G_N^0 \propto \phi^\alpha$, with α between 2.0 and 2.3 from solution studies. This concentration dependence of the second plateau modulus is reflected in the intensity of the low-frequency peak of the bimodal system. Viscosity and recoverable compliance, as well as the height of the peak, suggest that $\alpha \approx 2.2$ –2.3.

One should be able to go further and fit the whole dynamical loss curve, to account for the influence of one peak on the other. (This is an essential prelude to the treatment of samples where peaks are not well separated and, ultimately, of general polydispersed samples.) Various effects besides reptative escape from the entanglement tube must be included. One such effect is tube renewal. A description of this process has been suggested based on a Rouse-like relaxation,² and the extension to polydispersed systems was discussed here. Another treatment is based on tube enlargement,^{6,7} with any section of the polymer that has escaped by reptation up to a given time being regarded as no longer effective for entanglement. The former ideas are probably more accurate, but the latter are easier to apply when the system is polydispersed or the spectrum of disentanglement times is complex. The gross features of the experimental dynamic loss modulus curve agree with the predictions of both theories. More experiments are being performed. They should resolve the question of whether the remaining disagreements in the details of the fit are due to shortcomings of the models or to experimental difficulties. Indications are that some of the discrepancy can be eliminated with experiments designed to be more accurate at high frequencies.³

Another prediction of the theory worth testing carefully is the weak dependence of the product of zero-shear-rate viscosity, η_0 , and recoverable shear compliance, J_e^0 , on the relative volume fractions of the components of the mixture for a large enough concentration of longer molecules and a large ratio of molecular weights (both well above M_e).

Acknowledgment. We thank Dr. William W. Graessley for valuable discussions and for a critical reading of the manuscript.

Appendix

In this Appendix we present a few more details of the estimation of the relaxation spectrum for a chain of randomly distributed high- and low-friction segments, with the ratio of the friction constants very large. We will adopt a bead-spring model, which concentrates the friction at a point. There are ϕ_{fast} low-friction beads and ϕ_{slow} high-friction beads. Sequences of low-friction beads relax as if the bounding high-friction beads are stationary, which they effectively are on the time scale of the sequence's relaxation. For a low-friction bead connected by $n - 1$ springs, plus 2 springs to the high-friction beads, the relaxation rates are proportional to the eigenvalues of the $n \times n$ Rouse matrix

$$\begin{bmatrix} 2 & -1 & & & \\ -1 & 2 & -1 & & \\ & -1 & \ddots & & \\ & & & 2 & -1 \\ & & & -1 & 2 \end{bmatrix} \quad (A.1)$$

which are

$$\lambda_q^{(n)} = 4 \sin^2 \frac{\pi q}{2(n+1)}, \quad q = 1, \dots, n; n = 1, \dots \quad (A.2)$$

The density of states has a spike for each allowed value of q and n . The spike is not quite a δ function because of the small but finite coupling between fast sequences through slow segments. For a given n all values of q have the same weight (area under the peak). The weight associated with a given n is the probability of such a sequence in the chain

$$\phi_{slow} \phi_{fast}^n \quad (A.3)$$

For times $t \ll \tau_{slow}$ the relaxation factor from tube renewal is

$$R(t) \approx \phi_{slow} + \phi_{slow}^2 \sum_{n=1}^{\infty} \phi_{fast}^n \sum_{q=1}^n \exp \left[-\frac{2t}{\tau_{fast}} \sin^2 \frac{\pi q}{2(n+1)} \right] \quad (A.4)$$

The first term represents the ϕ_{slow} unrelaxed modes.

On the time scale for the slow segment relaxation the sequence of fast beads acts like a spring with effective spring constant¹⁴

$$\kappa_n = \frac{3k_B T}{(n+1)a^2} \quad (A.5)$$

where now $n = 0, 1, \dots$. The probability of a given n is given by eq A.3. The slow part of the spectrum corresponds to the relaxation of a chain of beads with friction ζ_{slow} and such stochastically assigned spring constants. A Monte Carlo estimate of a spectrum of slow tube renewal relaxation rates by the method of Dean⁹ is shown in Figure 3.

Registry No. Polybutadiene, 9003-17-2.

References and Notes

- (1) Struglinski, M. J.; Graessley, W. W. *Macromolecules* 1985, 18, 2630.
- (2) Graessley, W. W. *Adv. Polym. Sci.* 1982, 47, 67.
- (3) Rubinstein, M.; Colby, R., in preparation.
- (4) Doi, M.; Edwards, S. F. *J. Chem. Soc., Faraday Trans. 2* 1978, 74, 1789, 1802, 1818.
- (5) Doi, M. *J. Polym. Sci., Polym. Phys. Ed.* 1981, 19, 265.
- (6) Marrucci, M. *J. Polym. Sci., Polym. Phys. Ed.* 1985, 23, 159.
- (7) Viovy, J. L. *J. Phys. (Les Ulis, Fr.)* 1985, 46, 847.
- (8) Orwoll, R. A.; Stockmayer, W. H. *Stochastic Processes in Chemical Physics*; Shuler, K. E., Ed.; Wiley: New York, 1969.
- (9) Dean, P. *Proc. Phys. Soc., London* 1964, 84, 727.
- (10) Ferry, J. D. *Viscoelastic Properties of Polymers*, 3rd ed.; Wiley: New York, 1980.
- (11) Raju, V. R.; Menezes, E. V.; Graessley, W. W.; Fetters, L. J. *Macromolecules* 1981, 14, 1668.
- (12) Kelly, F. N.; Bueche, F. *J. Polym. Sci.* 1961, 50, 549.
- (13) Evans, K. E.; Edwards, S. F. *J. Chem. Soc., Faraday Trans. 2* 1981, 77, 1913.
- (14) Helfand, E. *Photophysical and Photochemical Tools in Polymer Science*; Winnik, M. A., Ed.; Reidel: Dordrecht, Holland, 1986.
- (15) Rubinstein, M.; Helfand, E. *J. Chem. Phys.* 1985, 82, 2477.